Our underlying assumption has been that configuration mixing would improve the spacing, but not change the order of levels. This has now been conclusively proved by Wathne and Engeland in the ^{24}Mg case.[10] They found that by gradually expanding the basis, the same order (the wrong one) consistently appears in the ^{24}Mg low levels, while the spacing is almost doubled. (The calculation was made with a Gaussian Rosenfeld potential.) As for the effective interaction, the main unorthodox feature in our assumption is the dropping of both the spin and the isotopic spin exchange. This assumption is however not so unrealistic as it may seem, since it is based on recent theoretical results of Parikh and Bhatt.[9] Their analysis of the effective residual interaction of Kuo and Brown[11] showed that the latter's matrix elements have in fact a Majorana exchange character. Finally the strength of the effective interaction has been derived from the excitation energy of the first excited ^{20}Ne state because detailed calculations show[12,13] that this value is hardly affected by configuration mixing.

[10] K. Wathne and T. Engeland, Nucl. Phys. **A94**, 129 (1967).

[11] T. T. S. Kuo and G. E. Brown, Nucl. Phys. **85**, 40 (1966).
[12] C. Abulaffio, Nucl. Phys. **81**, 71 (1966).
[13] J. Flores and R. Perez, Phys. Letters **26B**, 55 (1967).

PHYSICAL REVIEW VOLUME 181, NUMBER 4 20 MAY 1969

Statistical Theory of Nuclei. II. Medium and Heavy Nuclei*

K. A. Brueckner, J. R. Buchler, R. C. Clark, and R. J. Lombard†
Department of Physics and Institute for Pure and Applied Physical Sciences, University of California, San Diego, La Jolla, California 92037

(Received 30 December 1968)

The total energies of finite nuclei are expressed as a functional $E[\rho_p, \rho_n]$ of the local proton and neutron densities ρ_p and ρ_n. The binding energies and densities of any nucleus are found by minimizing $E[\rho_p, \rho_n]$ with respect to ρ_p and ρ_n separately. The potential-energy functional is initially derived from a nuclear matter calculation but later adjusted to reproduce experimental binding energies. Results for light nuclei have already been reported, and here the calculation is extended to medium and heavy nuclei. Binding energies and mean radii are well reproduced but surface thicknesses are too large and rms radii too small.

I. INTRODUCTION

THE idea of deriving bulk properties of nuclei by means of statistical methods goes back to the earlier days of nuclear physics. The main task consists of reproducing the binding energies, the sizes, and the shapes of nuclei without appealing to a microscopic description. Remarkable results have already been recorded within the framework of the Thomas-Fermi approximation using simple nuclear forces. Improvements in our understanding of the nucleon-nucleon interactions, as well as in the description of many-fermion systems, allow us to accomplish the program with greater accuracy and more confidence in the theoretical background. The Thomas-Fermi theory, for instance, has been recently reviewed in detail by Bethe,[1] assuming realistic nuclear forces with a repulsive core, which ensured its validity in the nuclear case.

The presence of a shell structure may well require the use of Hartree-Fock-like theories rather than statistical approaches. This is obviously the case for observables strongly depending on single-particle states. As an example, the shell-model potential experienced by a particle inside the nucleus is hardly given by a statistical expression. Nevertheless, solving Hartree-Fock-type equations results in a tedious computation, especially if use is made of a realistic two-body force, for which the Brueckner-Goldstone formalism has to be introduced. Thus, it remains worthwhile to derive general properties by means of more practical methods.

Another reason for dealing with statistical theories has been pointed out by Myers and Swiatecki.[2] It is essential to separate liquid-drop and shell effects in the semiempirical mass formula, in order to extrapolate the mass formula and to investigate heavy and superheavy nuclei. Higher-order corrections to the usual Bethe-Weizsäcker expression, arising from the surface symmetry energy, curvature effects, or exchange Coulomb energy, are difficult to extract from the actual

* Research supported by the U.S. Atomic Energy Commission under Contract No. AT(11-1)-GEN-10, P.A. 11.

† Present address: Institut de Physique Nucléaire, Division de Physique Théorique, laboratoire associé au CNRS, 91-Orsay, France.

[1] H. A. Bethe, Phys. Rev. **167**, 879 (1968), in which references to earlier works can be found as well as in Ref. 5; see also *Proceedings of the International Conference on Nuclear Physics, Gatlingsburg, Tenn., 1966* (Academic Press Inc., New York, 1967).

[2] W. D. Myers and W. J. Swiatecki, Nucl. Phys. **81**, 1 (1966); see also W. D. Myers and W. J. Swiatecki, Arkiv Fysik **36**, 343 (1967); W. D. Myers, University of California Radiation Laboratory Report No. UCRL-17725, 1967 (unpublished).

data. A statistical treatment is helpful in establishing these corrections.

In the present work we apply the energy-density formalism to finite nuclei. The basic idea is to express the total energy of the many-nucleon system as a functional $E[\rho(r)]$ of the local density $\rho(r)$

$$E[\rho(r)]\cong(\psi,H\psi) \tag{1}$$

by means of an extended Thomas-Fermi model. Then the variational method for finding the ground state of the system reduces to a minimization with respect to $\rho(r)$.[3] The functional of the potential energy is derived from a nuclear matter calculation with variable neutron excess carried out by Brueckner *et al.*[4] Effects of the finite range of the nuclear forces are included through a density gradient correction which takes care of the density variation at the nuclear surface. Its numerical coefficient is kept as a phenomenological parameter to be adjusted to the experimental data.

In a previous paper[5] (hereafter referred to as I) we have reported results concerning a first attempt in which proton and neutron densities have been assumed proportional. The calculations were therefore limited to light nuclei, essentially to nuclei with zero neutron excess. Our purpose is to investigate the effects of relaxing the proportionality between the two fermion densities, and to extend the calculations to medium and heavy nuclei. As we shall see in Sec. III, the differences between proton and neutron distributions do not significantly affect the binding energies or the rms of the mass radius. In Sec. III all constants other than η are the same as in I, allowing a connection to be made with the results in that paper.

Section IV is devoted to a study of nuclei using the differential-equation approach. In this section we also allow an adjustment of the saturation curves in order to obtain better binding energies. Conclusions are given in Sec. V.

II. MODEL

A detailed derivation of our energy functional has already been given in I, so that we will merely review the most important arguments and discuss a few points. The total energy is expressed by

$$E[\rho]=\int\mathcal{E}[\rho(r)](dr)^3, \tag{2}$$

with

$$\mathcal{E}[\rho]=\tfrac{3}{5}(\hbar^2/2M)(\tfrac{3}{2}\pi)^{2/3}\tfrac{1}{2}[(1-\alpha)^{5/3}+(1+\alpha)^{5/3}]\rho^{5/3}+\rho V(\rho,\alpha)+\tfrac{1}{2}e\rho_p\phi_C-0.7386e^2\rho_p^{4/3}+(\hbar^2/8M)\eta(\nabla\rho)^2 \tag{3}$$

and

$$\rho(r)=\rho_p(r)+\rho_n(r).$$

The densities are subject to the conditions

$$\int\rho_p(r)\,(dr)^3=Z,\qquad\int\rho_n(r)\,(dr)^3=N.$$

The neutron excess is defined by

$$\alpha(r)=[\rho_n(r)-\rho_p(r)]/[\rho_n(r)+\rho_p(r)] \tag{4}$$

and reduces to $(N-Z)/A$ if ρ_p and ρ_n are proportional.

The first term in (3) represents the kinetic energy and is simply taken from the Thomas-Fermi theory. According to Bethe,[1] this is a good approximation as long as $\rho(r)\gtrsim 0.17\rho_0$, ρ_0 being the normal density of nuclear matter. The so-called Weizsäcker correction, which is of the form $\xi(\nabla\rho)^2/\rho$, is supposed to improve the Thomas-Fermi expression in accounting for the kinetic surface energy. The value of the parameter ξ has been derived by various authors in the case of an infinite fermion system weakly perturbed by a density-coupled interaction and found to be $\frac{1}{9}$ (see the Appendix of I). The same value comes out in the case of the semi-infinite medium perturbed by a ripple potential.[6] However, it has been shown by Swiatecki[7] that in the semi-infinite case, for any reasonable potential, the kinetic energy at the surface is overestimated by the Thomas-Fermi approximation. This result has been confirmed recently by Moszkowski.[8] It means that the quantity ξ cannot be taken as a constant at the surface and should even change sign. The failure of the Weizsäcker approximation at the nuclear surface may be attributed to the fact that, in contrast to an infinite system, the nucleons are in bound states so that the kinetic energy of each of them becomes negative at large distances. For this reason we have omitted the Weizsäcker correction in this work.

A more sophisticated way to introduce surface corrections to the Thomas-Fermi theory has been suggested by Nagvi.[9] In his approach the starting point consists of the Hartree-Fock equations, and the surface corrections turn out to be sensitively dependent on the shape of the density distribution. This possible improvement, however, has not been considered in the present work.

The second term in (3) represents the potential energy

$$V(\rho,\alpha)=b_1(1+a_1\alpha^2)\rho+b_2(1+a_2\alpha^2)\rho^{4/3}+b_3(1+a_3\alpha^2)\rho^{5/3}. \tag{5}$$

[3] P. Hohenberg and W. Kohn, Phys. Rev. **136,** B864 (1964); L. J. Sham and W. Kohn, *ibid.* **145,** 561 (1966).

[4] K. A. Brueckner, S. A. Coon, and J. Dabrowski, Phys. Rev. **168,** 1184 (1968).

[5] K. A. Brueckner, J. R. Buchler, S. Jorna, and R. J. Lombard, Phys. Rev. **171,** 1188 (1968).

[6] L. Wilets and S. A. Moszkowski (private communication from S. A. Moszkowski); see also, D. S. Koltan and L. Wilets, Phys. Rev. **129,** 880 (1963).

[7] W. J. Swiatecki, Proc. Phys. Soc. (London) **64A,** 226 (1951).

[8] S. A. Moszkowski, Bull. Am. Phys. Soc. **13,** 628 (1968); and (private communication).

[9] M. A. Nagvi, Nucl. Phys. **10,** 256 (1959).

The coefficients b_i and a_i were initially derived from the nuclear matter calculation with variable neutron excess by Brueckner *et al.*[4] The precision of the fit to the saturation curves is better than 1% for small α. These coefficients were later adjusted to give better nuclear binding energies for all A and Z with a constant η. A discussion of this is given in Sec. IV.

The direct and exchange Coulomb energy are given by the third and the fourth term of (3), respectively. The Coulomb potential is defined as

$$\phi_C = e\int \frac{\rho_p(r')}{|\mathbf{r}-\mathbf{r}'|}\,(dr')^3. \tag{6}$$

The inhomogeneity correction, taking care of the decrease of the density at the nuclear surface, is expressed by the last term of (3). As shown in I, its analytical form can be derived from the gradient expansion of the potential energy, the long-range part of the two-body interaction only being considered. The coefficient η is taken in our work as a phenomenological parameter. It is, in principle, related to the long-range part of the potential and Bethe[1] gives a prescription for evaluating it. He suggests considering the $^1S_0$ part of the potential only and subtracting the OPEP contribution. This is not a general procedure and cannot be followed in the case of the Gammel-Thaler potential. However, in choosing a simple static force reproducing approximately our saturation curve for zero neutron excess, we get a value of η which is in rough agreement with the one we are using.

Another difficulty in the evaluation of η arises from the self-consistency requirement between the G matrix and the single-particle potential of the intermediate states. This has been noticed by various authors[10] in Hartree-Fock calculations. In the present case, as advocated by Bethe,[1] the extension of the local density approximation should lead to a simple renormalization of η. This seems consistent with the fact that in the energy-density formalism the inner part of the nucleus is more or less considered as a piece of nuclear matter, so that the correction should primarily affect the surface. Nevertheless, it is a size effect influencing the whole nucleus and the method of taking this into account is not very clear at present.

Among different possibilities it may seem attractive to choose η such as to fit the surface energy term of the semiempirical mass formula. This is easily done in the one-dimensional nucleus neglecting the Coulomb energy. However, the coefficient of the $A^{2/3}$ term is determined from the actual nuclei in which the curvature effects are not negligible, and higher-order effects like the surface symmetry energy may well bring additional uncertainties. Therefore fitting η to give the binding energy of a nucleus seems a better choice.

[10] See S. Köhler, Phys. Rev. **137**, B1145 (1965); D. S. Koltan, *ibid.* **137**, B487 (1965); C. W. Wong, Nucl. Phys. **91**, 399 (1967).

Higher-order terms in the gradient expansion, above all the $(\Delta\rho)^2$ terms, are neglected. A calculation of this term showed it to be about 1% of the total binding energy, thus of the order of the accuracy of the method.

III. ANALYTIC DENSITY DISTRIBUTIONS

The ground-state density distributions are calculated either by solving the Lagrange-type coupled differential equations associated with (2) or by a variational method in which use is made of appropriate trial functions for $\rho_p(r)$ and $\rho_n(r)$. The differential equations require a four-parameter search [or three if $\rho_n(r)$ and $\rho_p(r)$ are assumed proportional]. However, for heavy nuclei the solutions tend to be mathematically unstable and the variational method provides a convenient tool in seeking approximate solutions. The two minimization processes yield results in very close agreement.

For light nuclei, the best trial function was found to be a so-called modified Gaussian with a cubic polynomial. This form remains the best for medium and heavy nuclei, but the results are slightly improved by replacing the cubic term by a fourth-order one. The analytical expression is then

$$\rho_{n,p}(r) = \rho_0(1+pr^2+tr^4)\{1+\exp[(r^2-R^2)/b^2]\}^{-1}, \tag{7}$$

ρ_0 being determined by the condition on the number of protons and neutrons, respectively, There are two sets of four parameters (R, b, p, and t) to be varied. Investigations of eight-dimensional surfaces are generally very much involved. The weakness of the proton-neutron coupling simplifies the calculation, however, since it is possible to proceed by iteration, varying one set of parameters at each step. The convergence is quick enough so that the final result is reached after a small number of iterations. Within each iteration, one parameter is varied while the three others are kept fixed until the required precision is obtained for all four parameters. As initial values one may choose the parameters obtained for proportional densities. Note that the parameter t is negative. Therefore the densities are set equal to zero once they become negative.

As far as the analytical form of our trial functions is concerned, it is interesting to note that a so-called three-parameter Fermi distribution is not sufficiently general. A fourth-order term is necessary to bring the binding energy into agreement with experiment or to approach the solution of the differential equations with a sufficient accuracy. However, even with a fourth term the Fermi distribution seems to have a too large surface thickness and is asymmetric with respect to the point where the density reaches half of its central value. This result was also apparent in the differential-equation solution and has been found by Bethe.[1] It is probably a property of the Thomas-

TABLE I. Characteristic results of the variational method for separate proton and neutron densities using the theoretical saturation curves of Ref. 4. $\eta=8$, except in the case of Pb^{208} (b), for which $\eta=7$. Units are MeV and F. Experimental values are taken from Refs. 12–14. BE denotes total binding energy.

	Present work						Experimental			
	$-BE$	r_p	$r_{p,0.5}$	t_p	r_n	t_n	$-BE$	r_p	$r_{p,0.5}$	t_p
Ca^{40}	339	3.12	3.64	2.42	3.07	2.71	342	3.50	3.58	2.65
Ca^{48}	412	3.20	3.80	2.38	3.30	2.95	416	3.49	3.74	2.30
Sn^{116}	961	4.28	5.27	2.22	4.34	2.65	989	4.50–4.55	5.27–5.28	2.37–2.4
Pb^{208} (a)	1543	5.18	6.54	2.04	5.29	2.55	1636	5.39–5.55	6.48–6.7	2.0–2.35
Pb^{208} (b)	1582	5.18	6.61	1.95	5.30	2.35				

Fermi approximation, since calculations with simple potentials yield a more symmetric surface.[11] Electron scattering data are also fitted best by symmetric surfaces. These anomalies are in both the proton and neutron densities and cannot be overcome by choosing a different analytical form for each of them.

Another convenient function has been proposed by Bethe and Elton[12] and proved to yield very satisfactory results in fitting electron scattering and muonic x-ray data in Pb^{208}. For protons it is given by

$$\rho_p(r)=\rho_0[1+p(r^2/R^2)]\{1-\tfrac{1}{2}\exp[(r-R)/n]\}^2, \quad r<R$$
$$=\rho_0(1+p)\tfrac{1}{4}\exp[-\gamma(r-R)], \quad r>R. \quad (8)$$

Incidentally, the fourth parameter γ is determined by fitting the binding energy. We have tried a similar expression, namely,

$$\rho(r)=\rho_0(1+pr^2+tr^4)\{1-\tfrac{1}{2}\exp[(r-R)/b]\}. \quad (9)$$

This yields results quite comparable to those of the modified Gaussian.

In order to check our model and to investigate effects of the nonproportionality between proton and neutron densities systematically, the energies and densities of Ca^{40}, Ca^{48}, Sn^{116}, and Pb^{208} were calculated. This choice is dictated in part by the existing experimental data on charge distributions. No equivalent data are available for neutron distributions (except for Pb^{208}, as we shall see later). The results are listed in Table I and the corresponding densities are plotted in Figs. 1–4. We denote by r_p and r_n the rms of the proton and neutron radius, respectively, $r_{0.5}$ is the half-density radius, t_p and t_n are the proton and neutron surface thicknesses (defined in the usual way, as the distance in which the density falls from 90 to 10% of the central value). The calculation has been made for $\eta=8$; in the case of Pb^{208} we also quote values corresponding to $\eta=7$ for comparison.

As we can see, the experimental situation is fairly well reproduced by the model. The experimental binding energies are taken from the "1964 mass table,"[13] whereas data concerning the charge distributions are

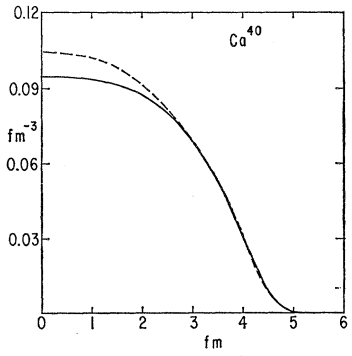

FIG. 1. Ca^{40}: proton (solid line) and neutron (dashed line) density distributions obtained using the variational method and the theoretical saturation curves of Ref. 4.

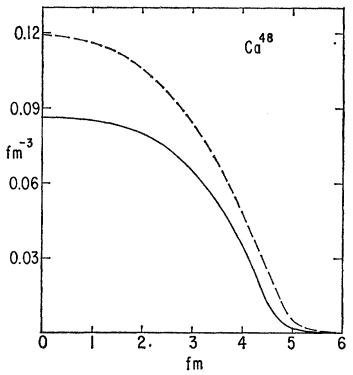

FIG. 2. Ca^{48}: proton (solid line) and neutron (dashed line) density distributions obtained using the variational method and the theoretical saturation curves of Ref. 4.

[11] S. A. Moszkowski (private communication).

[12] H. A. Bethe and L. R. B. Elton, Phys. Rev. Letters **20**, 745 (1967).

[13] J. H. E. Mattauch, W. Thiele, and A. H. Wapstra, Nucl. Phys. **67**, 1 (1965).

derived from the work of Hofstadter and Collard[14] as well as from Frosch *et al.*[15] The rms of the proton radius is systematically smaller than experiment by $\sim$0.3 F. The proton-size correction, which is of the order of 0.1 F at most and is not included here, is not sufficient to account for this discrepancy. This may, in part, be due to the fact that the Brueckner-Coon-Dabrowski calculation saturates nuclear matter for zero neutron excess at a density of $k_F \cong 1.44$ F^{-1}, as compared with the experimental value of 1.36 F^{-1} obtained from the central density of heavy nuclei, but may also be due to an inability of the model to reproduce the detailed structure of the distributions.

In the case of Pb^{208} the change in η does not affect the results very much: Lowering η from 8 to 7 increases the binding energy and decreases the surface thicknesses by $\approx 5\%$.

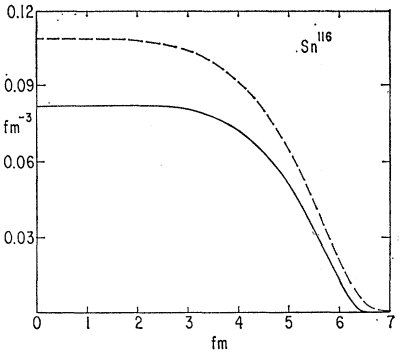

FIG. 3. Sn^{116}: proton (solid line) and neutron (dashed line) density distributions obtained using the variational method and the theoretical saturation curves of Ref. 4.

Finally, we would like to discuss the symmetry energy, i.e., the variation of the binding energy against the neutron excess within an isobaric set of nuclei. The calculation has been performed for $A=48$, 116, and 208 nuclei and the results are shown in Fig. 5. The well-known parabolic shape of the function $E_B(Z)$ is reproduced, but the fit to experiment is not very good. For this reason and in order to fit the total binding energies better, the constants in the potential energy and the parameter η were adjusted as described in Sec. IV. The binding energies were obtained by solving the differential equation with the proton and neutron densities treated separately. Figure 5 also shows the results obtained after varying the parameters. One should keep in mind that the energy differences between two isobars is small and that shell effects are expected to be important. It is the shell closure at $Z=50$, for instance, which makes the binding energy of Sn^{116} lower than that of Cd^{116}.

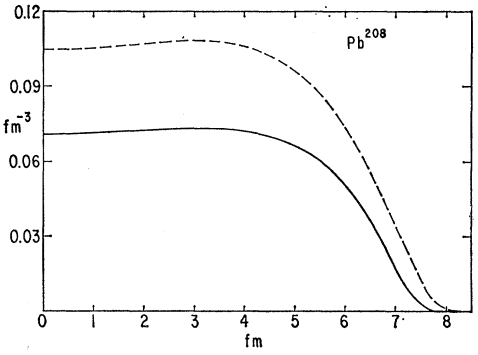

FIG. 4. Pb^{208}: proton (solid line) and neutron (dashed line) density distributions obtained using the variational method and the theoretical saturation curves of Ref. 4.

IV. DIFFERENTIAL-EQUATION METHOD

The first functional derivatives of $E[\rho]$ with respect to $\rho_n(r)$ and $\rho_p(r)$ are zero when $E[\rho]$ is minimized. These relations give directly a pair of equations, the

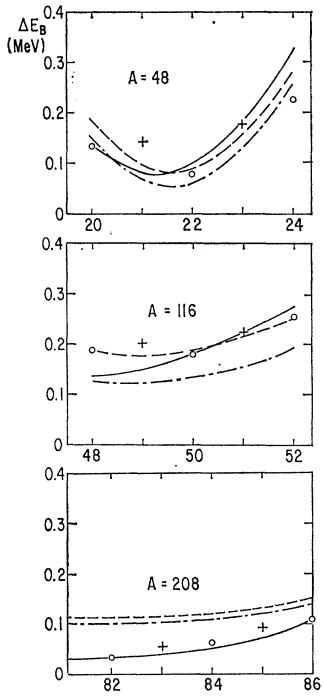

FIG. 5. Symmetry energies: The binding energies as a function of Z are plotted for $A=48$, 116, and 208 isobars. The experimental points are the circles and crosses. The solid lines are the results obtained with the saturation curves of Ref. 4 normalized to the binding energy of Ca^{48}, Sn^{116}, and Pb^{208} in each case. The dot-dashed lines are the results without normalization obtained with the adjusted saturation curves. The dashed lines are obtained from the liquid-drop part of the mass formula of Myers and Swiatecki (Ref. 2).

[14] H. R. Collard, L. R. B. Elton, and R. Hofstadter, in *Nuclear Radii*, edited by H. Schopper, Landolt-Börnstein (Springer-Verlag, Berlin, 1967), New Series, Group I, Vol. 2.

[15] R. F. Frosch, R. Hofstadter, J. S. McCarthy, G. K. Nodelke, K. J. Van Oostrum, M. R. Yearian, B. C. Clark, R. Herman, and D. G. Ravenhall (to be published).

solutions of which are the exact density functions for minimum $E[\rho]$. In principle, therefore, the differential-equation approach leads to better solutions than the variational approach, since no *a priori* assumptions about the general shape of the densities have to be made. In practice, however, the physical boundary conditions may be impossible to satisfy (because of breakdown of $E[\rho]$, for example) and the presence of singularities in the equations imposes the need for cutoffs on the solutions, introducing uncertainties and errors.

Initially a surface symmetry energy term was included in $E[\rho]$, although it is a small contribution to the total energy, for this leads to symmetry between $\rho_n(r)$ and $\rho_p(r)$ and allows two boundary conditions to be imposed on each of them. The term included was of the form

$$\theta(\hbar^2/8M\eta)[\nabla(\rho_n-\rho_p)]^2,$$

where θ was a constant taken to be equal to the ratio of the coefficient of α^2 in $V(\rho,\alpha)$ to $V(\rho,0)$ when $\rho=0.2$. The differential equations to be solved are then

$$\nabla^2\rho_p=(M/\eta\hbar^2)[D(\rho_p,\rho_n)-(1/\theta)F(\rho_p,\rho_n)], \quad (10)$$

$$\nabla^2\rho_n=(M/\eta\hbar^2)[D(\rho_p,\rho_n)+(1/\theta)F(\rho_p,\rho_n)]. \quad (11)$$

The functions D and F are given by

$$D(\rho_p,\rho_n)=\partial\mathcal{E}(\rho)/\partial\rho_n+\partial\mathcal{E}(\rho)/\partial\rho_p-(E_n+E_p), \quad (12)$$

$$F(\rho_p,\rho_n)=\partial\mathcal{E}(\rho)/\partial\rho_n-\partial\mathcal{E}(\rho)/\partial\rho_p-(E_n-E_p), \quad (13)$$

where E_n and E_p are Lagrange multipliers enabling the particle number conditions to be satisfied. It was found, however, that the solutions to the coupled equations (10) and (11) were extremely unstable and the boundary conditions could not be satisfied. Therefore the surface symmetry term was dropped from the energy functional (and added into the total energy later as a perturbation) and the simplified set of equations

$$\nabla^2\rho=(2M/\eta\hbar^2)D(\rho_p,\rho_n), \quad (14)$$

$$F(\rho_p,\rho_n)=0 \quad (15)$$

were solved instead. [In practice, it was found to be simpler to replace Eq. (15) by a differential equation $dF/dr=0$ and use $F=0$ as a boundary condition at $r=0$.] This meant that one less parameter had to be hunted, making the solution rather easier, but also meant that one less boundary condition could be met, and hence that the solutions were less satisfactory. The boundary condition that was dropped was the condition that the derivative of ρ_p should vanish as ρ_p tended to zero at the edge of the nucleus. Note that the energy functional $E[\rho]$ breaks down at the edge of the nucleus for two reasons: (a) The Thomas-Fermi approximation fails for low densities, and (b) at the edge of the nucleus the neutron-to-proton ratio becomes very large, α tends to unity, and the potential $V(\rho,\alpha)$ is not accurate for large α. Indeed, a pure neutron gas is unbound. Thus the boundary condition at the edge of the nucleus can only approximate to the physical condition. In this work, the boundary condition imposed was that the derivative of the total density should vanish at the edge of the nucleus, since this imposes something akin to an exponential tail on the density. However, the tails of our solutions should only be regarded as an indication of the behavior of the density distribution and not treated with certainty. Indeed, the variational solution probably reproduces this region better than the differential-equation solution.

When solving Eqs. (14) and (15), it was, of course, also necessary to solve Poisson's equation for the Coulomb potential. The linearity of Poisson's equation means that the solutions were independent of the assumed value of $\phi_C(0)$; only the sum of $\phi_C(r)$ and (E_n-E_p) occurs in Eq. (15). $\phi_C(0)$ is known when $\rho_p(r)$ has been found and the total energy may be then calculated correctly and (E_n-E_p) adjusted.

The three parameters $\rho(0)$, E_p, and E_n were hunted by using Newton's method for three variables. For light nuclei convergence was extremely rapid, but for heavier nuclei, particularly those exhibiting a bottleneck effect, reasonable starting values were found to be necessary before convergence was obtained because of a tendency for the bottleneck to build up. The solutions are unstable against a rapid increase in total density when the density rises above a certain value dictated by E_n and E_p. This is almost certainly connected with the assumed form of $V(\rho,\alpha)$ and is not a physical instability.

As mentioned at the end of Sec. III, the binding energies of large nuclei and the shape of the $E_B(Z)$ curve could not be satisfactorily reproduced with a constant value of η. Nor was it sufficient to change simply the depth of minimum in the saturation curve. Lowering the minimum from -15.3 to -16.3 MeV enabled us to fit E_B for all A with good accuracy with $\eta=10.8$ but the dependence of E_B on Z was still incorrect. The symmetry energy[4] ϵ_{sym} in $V(\rho,\alpha)$ needed to be increased from 56 to 68 MeV to give substantially better agreement for $E_B(Z)$. With the saturation curve minimum taken at -16.6 MeV and $\eta=12.0$, then the binding energies of all nuclei could be well reproduced. These adjusted values are interesting since they do not agree with the values in the mass formula of Myers and Swiatecki,[2] which are -15.5 MeV for nuclear matter and an ϵ_{sym} of 55 MeV. Moreover, the charge distributions appear to have a worse shape than before when compared to the experimental data. These results are discussed in the next section.

V. DISCUSSION

The present work, together with the results recorded in I, shows the ability of the energy-density formalism

TABLE II. Binding energies and separation energies in MeV after adjustment of the saturation curves. Experimental results and the theoretical estimates of Myers and Swiatecki (Ref. 2) and Köhler (Ref. 18) are also shown. The shell corrections have been subtracted out of the Myers-Swiatecki mass formula.

	Binding energies per particle				E_p		E_n	
Nucleus	Expt	Myers-Swiatecki (liquid drop)	Köhler	Present work	Expt	Present work	Expt	Present work
O^{16}	−7.98	−7.54	−8.75	−7.50	−12.13	−7.46	−15.67	−10.81
Ca^{40}	−8.55	−8.47	−8.72	−8.48	−8.34	−5.44	−15.73	−12.57
Ca^{48}	−8.67	−8.62	...	−8.65	−15.26	−13.09	−9.93	−6.18
Sn^{116}	−8.53	−8.51	...	−8.57	−9.11	−6.90	−9.39	−8.09
Ce^{140}	−8.39	−8.34	−7.79 (Ba^{138})	−8.39	−8.01	−7.61	−9.06	−6.69
Pb^{208}	−7.87	−7.80	−7.66	−7.79	−8.04	−6.67	−7.38	−5.08
Pu^{246}	−7.51	−7.50	...	−7.45	...	−6.68	−5.97	−4.00
114^{298} Prop. densities	...	−7.12	...	−6.90	...	−4.03	...	−4.03
114^{298} Separate densities	...	−7.12	...	−7.02	...	−4.05	...	−4.23

to reproduce properties of the finite nucleus. As far as the bulk properties are concerned, namely, the binding energy and the size and shape of the mass distribution, the calculation can be performed to a sufficient accuracy in assuming a constant neutron excess. This reduction of the number of independent variables leads to an appreciable simplification in the minimization process. Nevertheless, details of the proton and neutron distributions can only be studied in varying ρ_p and ρ_n separately.

Tables II and III compare our results with a very recent self-consistent field calculation by Köhler.[16] Here the comparison is particularly interesting, because Köhler is using an effective K matrix. The interaction he used was proposed by Seyler and Blanchard,[17] and was adjusted to reproduce the mass-formula parameters of Myers and Swiatecki.[2] The Köhler binding energies, however, contain a small uncertainty since the correction for the self-consistency requirement between the K matrix and the single-particle energies is not included. The major differences lie in the size of the nuclei, which is larger in the self-consistent field

TABLE III. Proton and neutron radii and surface thicknesses in F found using the revised saturation curves. Note that the surface thicknesses are too large and the rms radii too small.

	Neutron half-radius	Proton half-radius $r_{p,0.5}$		rms charge radius r_p		Surface thickness radius		rms mass radius	
Nucleus	$r_{n,0.5}$	Expt	Calc	Expt	Calc	Expt	Calc	Köhler	Present work
O^{16}	2.65	2.70–2.74	2.65	2.75–2.71	2.56	1.83–2.05	2.44	2.56	2.55
Ca^{40}	3.52	3.58	3.59	3.50	3.24	2.65	2.80	3.36	3.23
Ca^{48}	3.79	3.74	3.74	3.49	3.29	2.30	2.75	...	3.38
Sn^{116}	5.17	5.27–5.28	5.20	4.50–4.55	4.32	2.37–2.40	2.78	...	4.37
Ce^{140}	5.54	...	5.55	...	4.56	...	2.69	5.08 (Ba^{138})	4.62
Pb^{208}	6.43	6.48–6.70	6.43	5.39–5.55	5.16	2.0–2.35	2.43	5.77	5.24
Pu^{246}	6.84	...	6.83	...	5.43	...	2.29	...	5.53
114^{298} Prop. densities	7.33	...	7.33	...	5.85	...	2.52	...	5.85
114^{298} Separate densities	7.37	...	7.37	...	5.81	...	2.10	...	5.90

[16] H. S. Köhler (to be published).
[17] R. G. Seyler and C. H. Blanchard, Phys. Rev. **124**, 227 (1961); **131**, 355 (1963).

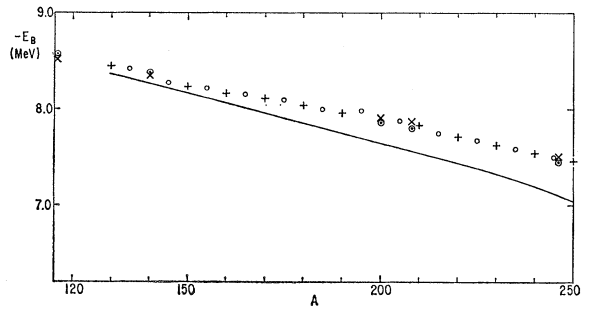

FIG. 6. Binding energies of nuclei with $\alpha=0.2$ plotted against A. The circles and upright crosses are experimental values. The solid line shows the result obtained for proportional neutron-proton densities with the theoretical saturation curves of Ref. 4 and $\eta=7.0$. Also shown are the experimental values (diagonal crosses) for Sn^{116}, Ce^{140}, Hg^{200}, Pb^{208}, and Pu^{246}, and the corresponding calculated energies (ringed dots) obtained with the saturation curves adjusted as described in Sec. IV and $\eta=12.0$.

calculation, and in the fact that, in contrast to the Thomas-Fermi result, the surface of semi-infinite nuclear matter is symmetric with respect to the half-density point.

When the saturation curves were adjusted to obtain better binding energies, the binding energies of two nuclei (Ca^{40} and Pb^{208}) were fitted to the liquid-drop part of their total energy. This energy was estimated from the empirical formula of Myers and Swiatecki,[2] and Figs. 5 and 6 show the results. Tables II and III give the new binding energies, rms charge radii, half-density radii, and charge surface thicknesses. For 114^{298} the results are compared with that obtained assuming ρ_p and ρ_n are proportional. It will be seen that enforcing this condition smooths out the bottleneck effect in ρ_p and also flattens the charge surface, since ρ_p now has to extend out with ρ_n. The binding energies of all nuclei investigated are now in close agreement with those of Myers and Swiatecki but we still have too large surface thicknesses and too small rms radii. Both of these results may be due to the fact that a statistical density is oversmooth and that there is an insufficiently sharp edge to the distribution. We have looked at the possibility of obtaining better values for the rms radii and surface thicknesses by adjusting the saturation curves further. Estimates show that large changes would be needed to obtain a fit to experimental data. For example, a change of the order of 100% in the curvature of the minimum would be needed to improve the surface thickness. A change of 25% in the value of the nuclear matter density would fit the rms radii but would make the half-radii too big. These large changes are not justified. A shell calculation is needed to reproduce the detailed structure of the distribution.

It is interesting to note that the surface energy coefficient, defined as

$$E_{\mathrm{surf}}A^{2/3}=E_{\mathrm{tot}}-E_{\mathrm{Coul}}-AE_{\mathrm{sat}}(\rho_0,\alpha),$$

only varies between 21.3 and 18.7 MeV over all the nuclei in Table II. The scatter can be attributed to the approximate treatment of the symmetry contribution. In the above expression, E_{Coul} includes both the direct and exchange Coulomb energies and $E_{\mathrm{sat}}(\rho_0,\alpha)$ is the minimum in the saturation curve at the appropriate α $[=(N-Z)/A]$ for the nucleus. One should also remark that with $\eta=12.0$ the gradient energy coefficient is in close agreement with the coefficient calculated by Bethe.[1] Bethe uses $B=24$ MeV, whereas our equivalent B is 24.9 MeV.

The neutron half-density radius is very close to the proton half-density radius especially for the heavier nuclei. But as will be seen from Figs. 1–4, the neutron's distribution extends about 0.2–0.5 F beyond the proton's, except for Ca^{40} and, more generally, for other nuclei having an equal number of protons and neutrons. This is in agreement with K-meson absorption experiments in nuclear emulsions in which evidence is found for the presence of a neutron excess at the surface.[18]

The energy-density formalism allows also a study of the mean potential experienced by the last bound nucleon as well as by a scattered particle in the static approximation. Therefore, it should be comparable to the usual Wood-Saxon potential. For a pure Thomas-Fermi calculation, the nuclear potential is given by

$$V_{n,p}(r)=E_{n,p}-\mathrm{const}\ \rho_{n,p}^{2/3}. \qquad (16)$$

The formula is no longer so simple if a gradient-type correction is applied to the kinetic energy but is approximately valid in the interior of the nucleus where the density is nearly flat. $V_{n,p}(r)$ is not a good shell-model potential for the deep particles but it is at least as good as a Wood-Saxon potential and is reasonable for the states near the Fermi surface, that is, for the last major shell.

The experimental result that the rms proton radius of Ca^{48} is less than that of Ca^{40} cannot be reproduced by the statistical model. However, part of the shift is seen, since the rms radius of Ca^{48} is less than would have been expected from an $A^{1/3}$ law. Also, the Ca^{48} proton surface thickness is less than that of Ca^{40}, in qualitative agreement with experiment. A calculation of shell effects based on the $V_{n,p}(r)$ does not fully account for the rest of the isotope shift.[19]

It has been suggested by Nolen, Schiffer, and Williams[20] that the energy of the isobaric analog state together with the charge radius may be used to calculate the radius of the neutron distribution. They applied

[18] D. H. Davis, S. P. Lovell, M. Osejthey-Barth, J. Sacton, and G. Schorochoff, Nucl. Phys. **B1**, 434 (1967); E. H. S. Burhop, *ibid.* **B1**, 438 (1967).

[19] K. A. Brueckner, Wing Fai Lin, and R. J. Lombard (to be published).

[20] J. A. Nolen, Jr., J. P. Schiffer, and N. Williams, Phys. Letters **27B**, 1 (1968); see also Ref. 21.

their method to Pb^{208} and found the neutron rms radius larger than the charge radius by 0.07 ± 0.03) F. This is in good agreement with our results in Table I. On the other hand, it is to be emphasized that we find that the proton half-density radius lies close to that of the neutrons. This point has been discussed by Bethe and Siemens.[21]

The charge densities of O^{16}, Ca^{40}, Sn^{116}, Ce^{140}, Pb^{208}, and Pu^{246} are plotted in Fig. 7, giving a good outline of the variation of the shape against the mass number. The "wine-bottle" effect only starts around $A=200$. A comparison of these curves with those of Figs. 1–4 shows the effect of altering the saturation curve parameters. In Fig. 7 the lack of a tail on the charge distributions for heavier nuclei can be seen. This stems directly from the choice of boundary conditions to Eqs. (14) and (15).

The energy-density formalism constitutes a very good tool for studying the existence of superheavy nuclei. For instance, the binding energy of the $_{114}X_{184}^{298}$, which is supposed to be the next closed- or semiclosed-shell nucleus, is of the order of 7.0 MeV/particle. Obviously shell effects are very important for such a large nucleus and have to be included in order to study the stability against spontaneous fission. Calculations along this line are now in progress, together with a study of the changes in density as the nucleus deforms.

The shape of the distribution especially at the surface shows that it is necessary to improve the energy functional. The tails of our densities are shorter than those of the Fermi-type functions used in analyzing

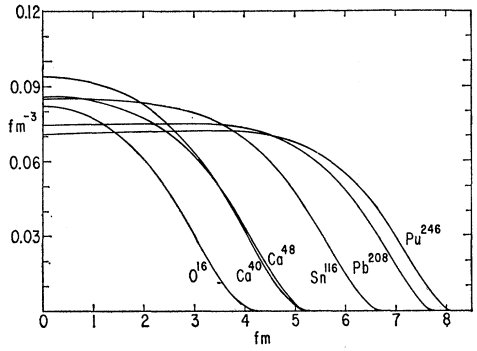

FIG. 7. Charge densities of nuclei obtained using the adjusted saturation curves. These curves should be compared with those of Figs. 1–4. The flatter shapes result from the increased gradient energy contribution.

[21] H. A. Bethe and P. J. Siemens, Phys. Letters **27B**, 549 (1968).

electron scattering data, or, as pointed out by Bethe,[1] at the point of the steepest slope, ρ is roughly 0.3 ρ_0, whereas it is 0.5 ρ_0 in case of a Fermi distribution. The Thomas-Fermi approximation is known to fail for densities lower than 0.15 ρ_0, that is, for a region which still contains an appreciable fraction of the particle number or, in other words, which contributes quite significantly to the total energy. We have also seen that this is a region of large α. In the case of Pb^{208} Bethe and Elton[12] have shown that both Fermi- and Thomas-Fermi-type distributions can reproduce electron scattering and muonic x-ray data. On the other hand, as remarked above, self-consistent field calculations favor Fermi distributions. It would be interesting to make further investigations to get more insight on this problem.

In summary, we have been able to reproduce the binding energies of nuclei from a mass formula that is fundamentally based in theory. The adjustments to the saturation curves described above are well within the errors inherent in the derivation of those curves and we can proceed with confidence in the formalism. Although our energy functional has to be improved to reproduce the charge distributions more consistently, the formalism has proved to be very useful in investigating nuclear structure. It can be substituted for the Hartree-Fock approximation each time one is looking for a gross structure rather than a microscopic description. This is the case, for instance, in heavy-ion scattering problems, where the energy functional can be used to calculate the scattering potential between two heavy ions.[22] How the results depend on the chosen nucleon-nucleon interaction is mainly expressed through the saturation curves. The Reid potential has been used by Bethe.[1] His results are in qualitative agreement with ours. However, the Reid potential does not give enough binding energy to nuclear matter, so that the potential energy had to be arbitrarily increased by 20%. This gives rise to the problem of whether the saturation curves have to be determined from a realistic static potential, which generally does not give enough binding energy, or from an effective interaction. The nonlocality of the interaction could be essential here and it would be very interesting to repeat the calculation with a more fundamental force based on meson-exchange theory in which the momentum dependence has been introduced with some care.[23]

[22] K. A. Brueckner, J. R. Buchler, and M. M. Kelly, Phys. Rev. **173**, 944 (1968).

[23] R. A. Bryan and Bruce L. Scott, Phys. Rev. **164**, 1215 (1967); L. Ingber, *ibid.* **174**, 1250 (1968).